Alzheimer's Research & Therapy

RESEARCH

Open Access

Tau seeding activity in the cerebrospinal fluid of Alzheimer disease patients predicts short-term cognitive decline

Ludivine Houzé[1], Marc Dhenain[2], Suzanne Lam[2], Fanny Petit[2], Stéphane Haïk[3], François Mouton-Liger[4], Jacques Hugon[4], Julie Dam[1], Claire Paquet[4], Ralf Jockers[1†] and Erika Cecon[1*†]

Abstract

Background Alzheimer disease (AD) clinical progression is highly heterogeneous, making its prediction essential for the development of effective therapies. The advancement of cognitive decline in AD is tightly linked to the spread of pathological tau protein aggregates in the brain, through tau seeding properties.

Methods We developed a cellular biosensor to measure tau seeding activity from cerebrospinal fluid (CSF) and human brain lysates. Longitudinal analysis of cognitive function was correlated with biosensor response.

Results Individuals with CSF exhibiting high or intermediate seeding activity experienced more rapid cognitive decline compared to those with low seeding. High tau seeding was associated with total and phosphorylated tau biomarkers in AD. The biosensor also predicts the potential of human AD brain lysates to induce tau aggregation upon experimental transmission in animal models.

Conclusions These results suggest that seeding activity might be a relevant biomarker to forecast AD pathogenicity and clinical progression.

Keywords Biosensors, Seeding, Spread, Tauopathy, Cognitive decline, Alzheimer, CSF, Biomarker

Background

Alzheimer disease (AD) is the most common age-related neurodegenerative disease, affecting more than 55 million people worldwide [1]. It is a heterogeneous condition, with remarkable inter-individual differences on clinical progression, making it crucial to enhance the accuracy of cognitive decline predictions to better stratify AD patients and improve the development of effective therapies. Pathological accumulation of hyperphosphorylated tau protein and aggregates of the amyloid beta peptide (Aβ) are the core molecular hallmarks of AD brain lesions. The molecular processes leading to their formation start decades before the appearance of clinical symptoms [2, 3]. Tau and Aβ-based biomarkers detected by brain imaging or measured in the cerebrospinal fluid

†Ralf Jockers and Erika Cecon are co-last authors.

*Correspondence:
Erika Cecon
erika.cecon@inserm.fr
[1]Université Paris Cité, CNRS, Inserm, Institut Cochin, Paris F-75014, France
[2]Laboratoire des Maladies Neurodégénératives, Université Paris-Saclay, CEA, CNRS, Fontenay-aux-Roses, France
[3]Sorbonne Université, Paris Brain Institute - ICM, INSERM, CNRS, AP-HP, Hôpital de la Pitié Salpêtrière, Paris, France
[4]Université Paris Cité, IHU reConnect, GHU AP-HP nord Hôpital Lariboisière, UMRS 1144 , Paris, France

(CSF) or plasma allows now a biological characterization of an AD continuum based on the presence/absence of three components: Aβ lesions (A), tau lesions (T), and neurodegeneration (N), comprising the A/T/N framework [4]. Pathological tau conformation is thought to spread from one neuron to another through prion-like seeding and propagation mechanisms [5], and the spreading of pathological tau in the brain, classified as Braak stages, displays strong correlation with cognitive decline in AD [6, 7]. This process requires seeding-active (or seeding-competent) tau species that can initiate the misfolding of normal tau proteins, ultimately leading to the oligomerization/aggregation cascade [8].

Tau seeding activity from *post-mortem* brain lysates from animal models of tauopathies, as well as from AD cases, can be detected using recently developed in vitro or cell-based assays [9–12]. These assays showed that, in animal models, seeding activity precedes the histological detection of tau aggregates in time [9]. Seeding activity also correlates well with the Braak stage of AD patients [11, 13]. A recent report described substantial person-to-person heterogeneity in tau seeding activity detected in *post-mortem* human brain lysates from AD patients, and suggested that this aspect might contribute to the observed clinical heterogeneity of the disease [14].

We have recently developed a series of highly sensitive and quantitative tau biosensors based on the enzyme complementation of nanoluciferase enzyme (NanoBit system) [15]. The NanoBit system display several advantages compared to previous biosensors, such as: high sensitivity; high-throughput and quantitative properties; large dynamic range; smaller size of fused Nluc proteins (SmBit: 1 kDa; LgBit: 18 kDa) compared to classical fluorescent proteins, minimizing the impact of the fusion protein on the function of the target protein; and straightforward procedure for data analysis. These tau biosensors detect robust tau seeding activity of brain lysates from the P301S transgenic mouse model of tau pathology (PS19), and allows precise quantification of inter-individual variability of their seeding potency [15]. In the present study, we applied the NanoBit-based tau biosensors to characterize tau seeding activity in human CSF samples from a clinical cohort followed-up longitudinally. The feasibility of detecting tau seeding activity in the CSF of living patients has been previously tested but led to controversial results [16]' [17]. We validated the biosensors by using *post-mortem* human brain lysates from two clinically distinct groups of sporadic AD patients, whose pathological properties were further evaluated by analysis of tau pathology induced upon their inoculation into the brain of an AD mouse model. Finally, we show that the seeding activity in the CSF might be a relevant parameter to define AD subpopulations and to predict the rate of cognitive decline. Being able to detect seeding activity from *ante-mortem* samples as biological fluids would be a breakthrough to help to define AD subtypes in vivo and to stratify subjects prior to clinical trials.

Table 1 Clinical characteristics from CSF samples donors

CHARACTERISTICS	NEUROLOGICAL CONTROLS (*N* = 30)	AD PATIENTS (*N* = 55)	*P*-VALUE
Age (years)	64.17 (7.1)	65.36 (7.2)	0.48
Male sex (%)	46.7	34.5	0.08
MMSE score (/30)[1]	27.48 (1.9)	19.27 (6.1)	< 0.0001****
APOE ε4 carrier %[2]	27	69	< 0.0001****
Abeta 40 (pg/mL)	11,562 (3095)	12,144 (3224)	0.31
Abeta 42 (pg/mL)	1437 (302.9)	719.5 (248.8)	< 0.0001****
P-tau 181 (pg/mL)	19.75 (14)	42.39 (20)	< 0.0001****
Total tau (pg/mL)	171.6 (44.3)	393.7 (159.6)	< 0.0001****

N, % or pg/mL (± S.D)

Statistic tests: Student *t* test; except Gender and APOE: contingency χ^2 test; **** $p < 0.0001$

[1] missing values = 6

[2] missing values = 6

Methods

Participants

The human CSF samples were collected at the Center of Cognitive Neurology, Lariboisière Hospital with approval by the Ethical Committee of Paris Diderot University Hospitals (CEERB Bichat University Hospital, Paris, France). Samples from 55 AD and 30 neurological control subjects were used in this study. Patients underwent a thorough clinical examination involving personal medical and family histories, neurological examination, neuropsychological assessment, CSF biomarker analysis, magnetic resonance imaging of brain structure as well as plasma and CSF biobanking. The diagnosis for each patient was made during multidisciplinary consensus meetings (by neurologists, neuropsychologists, neuroradiologist and biochemist) considering CSF results and according to validated clinical diagnostic criteria for AD. The individuals with no underlying neurocognitive disease and normal CSF biomarkers profile were enrolled as neurological controls. The cognitive follow up was mainly performed using Mini Mental test evaluation (MMSE). The main characteristics of the study population are presented in Table 1. Among the 55 AD patients from this study, 34 had one or several follow-up MMSE score measurements within three years.

Frozen human brain lysates (parietal cortex) from eight sporadic AD patients as well as two age-matched control individuals were collected from a brain donation program of the NeuroCEB and the CNR-prion brain banks. AD patients had a classical evolving form of the pathology (cAD), characterized by a disease duration of 5 to 8

years ($n = 4$), or a more rapidly evolving form (rAD) characterized by a disease duration of 6 months to 3 years ($n = 4$). Details of these lysates can be found in Table 2 and [18, 19]. Consent forms were previously signed by either the patients themselves or their next of kin, in accordance with French bioethics laws.

Sample preparation

The human CSF samples were centrifuged at 4 °C and stored at -80 °C within 4 h after lumbar punction. CSF biomarkers quantification (Aβ ratio ($A\beta_{42}/A\beta_{40}$), phosphorylated-tau (P-tau181) and total tau) were performed in the Biochemistry Unit (Lariboisière Hospital), using Innotest® ELISA (Fujirebio, Gent, Belgium). An ATN biological profile was defined for all included patients and neurological controls. Of note, established thresholds of these biomarkers for AD diagnosis are: $A\beta_{42} < 860$ (pg/mL); $A\beta_{42/40} < 0.08$; tau > 225 (pg/mL); and P-tau > 22 (pg/mL) [20].

Parietal cortex samples from each patient were individually homogenized at 10% weight/volume (w/v) in a sterile 1X Dulbecco's phosphate buffer solution in CK14 soft tissue homogenizing tubes at 5000 rpm for 20 s (Precellys®, Bertin technologies). We pooled brain homogenates by combining the four brain extracts from each AD group, as well as a control homogenate from the brains of two non-demented individuals (Ctrl). They were then sonicated on ice (5 s at 40% amplitude) and centrifuged at 3000 g for 5 min at 4 °C. The resulting supernatant was aliquoted in sterile polypropylene tubes and stored at -80 °C until use.

Transgenic mice

We used two mouse models in this study: the P301S (PS19), and the $APP_{swe}/PS1_{dE9}$ (C57Bl6 background) transgenic models. Brain lysates of the P301S (PS19) were prepared as previously described [15], and used as positive control, as the first characterization of these sensors were done using these samples [15]. Briefly, the cortex from five nine-months-old male heterozygous PS19 mice was rapidly removed after sacrificed and flash-frozen. Frozen tissue was lysed in PBS using a homogenizer, sonicated, and centrifuged (21,000 g, 15 min, 4 °C). The supernatant was aliquoted and stored at -80 °C until use.

The $APP_{swe}/PS1_{dE9}$ mouse model was used for the experiments involving the inoculation of human brain lysates, a model previously validated for this application [18]. Animals were inoculated with AD or Ctrl brain extracts at 2 months of age (details in the next section), and studied eight months after (8 months post-inoculation (mpi) $n_{Ctrl}=15$, $n_{AD1}=15$, $n_{AD2}=20$). At the time of the inoculation of the brain extracts, these mice did not have Aβ plaques. All $APP_{swe}/PS1_{dE9}$ mice were born and bred in our center (Commissariat à l'Energie Atomique, centre de Fontenay-aux-Roses; European Institutions Agreement #B92-032-02). All experimental procedures were conducted in accordance with the European Community Council Directive 2010/63/UE and approved by local ethics committees (CEtEA-CEA DSV IdF N°44, France) and the French Ministry of Education and Research (A17_083 authorization), and in compliance with the 3R guidelines. Animals were housed under standard environmental conditions (12 h light-dark cycle, temperature: 22 ± 1 °C and humidity: 50%) with *ad libitum* access to food and

Table 2 Patient characteristics of brain lysate donors

Patient					Neuropathology						
ID	Age	Gender	Disease progression (months)	Post mortem delay (hours)	Braak stage	Thal stage	CAA	α-synuclein	TDP43	Hippocampal sclerosis	PrPSc
Ctrl1	66	M	-	26	II	0	0	0	0	0	0
Ctrl2	76	M	-	NA	II	0	0	0	0	0	0
AD1a	79	F	78	48.6	V	5	Type2	0	0	0	0
AD1b	87	F	72	29	V-VI	4	Type1	0	0	0	0
AD1c	89	F	96	30.6	V	5	Type1	0	0	0	0
AD1d	71	M	66	54	VI	4	Type2	Amygdala	0	0	0
AD2a	84	F	6	79	V	4	Type2	0	0	0	0
AD2b	81	F	36	NA	V	5	Type1	0	0	0	0
AD2c	81	F	36	26	VI	4	0	0	0	0	0
AD2d	86	F	36	20.5	V	4	Type2	0	0	0	0

Age-matched classical slowly (cAD = AD1) and rapidly evolving (rAD = AD2) Alzheimer patients were selected based on disease duration (over or under 36 months) and neuropathological evaluation, including similar Braak and Thal stages. Brains were negative for α-synuclein, TAR DNA-binding protein 43 (TDP43), hippocampal sclerosis and pathological prion PrPSc. Two non-Alzheimer control individuals (Ctrl) were also included in this study. NA: not available

water. The design and reporting of animal experiments were based on the ARRIVE reporting guidelines [21]. Sample size was based on previous experiments for AD lesion induction in $APP_{swe}/PS1_{dE9}$ mice after inoculation of human brain with significance level of 5%, a power of 80%, and a two-sided test [22]. No animals were excluded from the study. SL was aware of initial group allocation, but further *post-mortem* analyses were performed blinded.

Stereotaxic inoculation of human brain homogenates

Two months-old $APP_{swe}/PS1_{dE9}$ were anesthetized by an intraperitoneal injection of ketamine (1 mg/10 g; Imalgène 1000, Merial) and xylazine (0.1 mg/10 g; 2% Rompun, Bayer Healthcare). Local anesthesia was also performed by a subcutaneous injection of lidocaine at the incision site (1 µl/g; 0.5% Xylovet, Ceva). Mice were placed in the stereotaxic frame (Phymep) and bilateral injections of brain samples were performed in the dorsal hippocampus (AP -2 mm, DV -2 mm, L +/- 1 mm from bregma). Two µl/site of sample were administered using 34-gauge needles and Hamilton syringes, at a rate of 0.2 µl/min. After the injection, needles were kept in place for 5 more minutes before removal and the incision was sutured.

Sample preparation for histology

$APP_{swe}/PS1_{dE9}$ mice were sacrificed at 8 mpi, with an intraperitoneal injection of a lethal dose of pentobarbital (100 mg/kg; Exagon, Axience). They were perfused intracardiacally with cold sterile 0.1 M PBS for 4 min, at a rate of 8 mL/min. The brain was extracted and post-fixed in 4% paraformaldehyde for 48 h at 4 °C, transferred into a 15% sucrose solution for 24 h and in a 30% sucrose solution for 48 h at 4 °C for cryoprotection. Serial coronal sections of 40 µm were performed with a microtome (SM2400, Leica Microsystem) and stored at -20 °C in a storing solution (glycerol 30%, ethylene glycol 30%, distilled water 30%, phosphate buffer 10%). Free-floating sections were rinsed in a 0.1 M PBS solution before use. Washing and incubation steps were performed on a shaker at room temperature unless indicated otherwise.

Immunohistochemistry for tau pathology

Tau was evaluated in the inoculated $APP_{swe}/PS1_{dE9}$ mice using AT8 antibody directed against hyperphosphorylated tau. Labelling was performed after a pre-treatment with EDTA 1X citrate (Diagnostic BioSystems®) for 30 min at 95 °C. All tissues were then incubated in 30% hydrogen peroxide (Sigma-Aldrich®) diluted 1/100 for 20 min to inhibit endogenous peroxidases. Blocking of non-specific antigenic sites was achieved over 1 h using a 0.2% Triton X-100/0.1 M PBS (Sigma-Aldrich®) (PBST) solution containing 4.5% normal goat serum or 5% bovine serum albumin. Sections were then incubated at 4 °C with the AT8 (Thermo MN1020B, 1/500) diluted in a 3%NGS/PBST solution for 96 h. After rinsing, an incubation with the appropriate biotinylated secondary antibody diluted to 1/1000 in PBST was performed for 1 h at room temperature, followed by a 1 h incubation at room temperature with a 1:250 dilution of an avidin-biotin complex solution (ABC Vectastain kit, Vector Laboratories®). Revelation was performed using the DAB Peroxidase Substrate Kit (DAB SK4100 kit, Vector Laboratories®). Sections were mounted on Superfrost Plus slides (Thermo-Scientific®). A cresyl violet counterstain was performed. All sections were then dehydrated in successive baths of ethanol at 50°, 70°, 96° and 100° and in xylene. Slides were mounted with the Eukitt® mounting medium (Chem-Lab®). Stained sections were scanned using an Axio Scan.Z1 (Zeiss® - Z-stack images acquired at 20× (z-stacks with 16 planes, 1 µm steps with extended depth of focus)). Image processing and analysis were performed with the ImageJ software. Quantification of neuritic plaques and NFTs was performed by manual counting on AT8 staining. A semi-quantitative analysis of neuropil threads (NT) was performed by assigning a severity score based on the intensity and extent of AT8-positive staining in each ROI. All quantifications were performed on adjacent slices between −0.34 mm and −4.36 mm from bregma. Five adjacent slices were analyzed. All ROIs were manually segmented using the Paxinos and Franklin neuro-anatomical atlas of mouse brain [23].

Cell culture and transfection

HEK293T (Sigma-Aldrich; RRID: CVCL 0063; authenticated by the provider) were maintained in Dulbecco's Modified Eagle's Medium (DMEM) Glutamax (Invitrogen) supplemented with 4.5 g/L glucose, 10% fetal bovine serum, 100 U/mL penicillin and 0.1 mg/mL streptomycin, at 37 °C (95% O_2, 5% CO_2). Cells were transfected with plasmid vectors coding for the NanoBit biosensors using jetPEI reagent, according to the supplier's instructions (Polyplus-transfection, New York, NY, USA). Alternatively, cells were transduced with lentivirus carrying the vectors coding for the same NanoBit biosensors (custom production by VectorBuilder GmbhH, Germany), to ensure more homogeneous expression.

NanoBit biosensor assay

NanoLuc® Binary Technology (NanoBiT, Promega) is a structural complementation reporter system composed of a Large BiT (LgBiT; 18 kDa) subunit and a small complimentary peptide. For the study of protein: protein interactions, the complimentary peptide is Small BiT (SmBiT; 11 amino acid peptide), which has been optimized to have low affinity for LgBiT [24]. The LgBiT and

SmBiT subunits are expressed as fusions to target proteins of interest and expressed in cells. When the two proteins interact, the subunits come together to form an active enzyme and generate a bright luminescent signal in the presence of substrate. Here, the tau biosensor comprises tau molecules fused to either LgBit or Smbit and expressed in HEK293T cells. In this work we used biosensor cells based on full length tau(P301L) (i.e. LgBit-Tau(P301L) and SmBit-(TauP301L) constructs), and the K18 fragment of tau(P301L), which is a 12 kDa peptide which sequence constitutes the full microtubule binding domain [25] (i.e. LgBit-K18(P301L) and SmBit-K18(P301L)). All biosensor constructs have also an HA tag. One day after transfection, cells were plated into white 96-well plates (Perkin Elmer Life Sciences, Waltham, MA) precoated with poly-L-lysine (Sigma-Aldrich) at a density of 2×10^4 cells/well. Cells were incubated with the test samples (human CSF: 0.5 µL per well; human brain lysates: 2.5 µg of total protein per well; mouse brain lysate: 1 µg of total protein per well), diluted in OptiMEM containing Lipofectamine 2000 reagent (Invitrogen) (1 µL lipofectamine per well in the final volume). All samples were sonicated prior to use. Basal condition is defined by OptiMEM-Lipofectamine mix without any test sample. All groups were assayed in triplicates. After 24 h incubation at 37 °C (95% O_2, 5% CO_2), cells were washed once with PBS, followed by addition of the NanoGloLiveCell substrate (1:20 dilution; Promega) and the bioluminescence signal was immediately recorded using the Envision plate reader (Perkin Elmer Life Sciences). The signal obtained was normalized by dividing it by the signal of the basal group (sensor cells in the absence of samples) to obtain an intra-assay Relative Luminescence signal (RLU).

Immunofluorescence microscopy

TauP301L biosensor cells were plated on coverslip previously coated with poly-L-lysine and treated with 1 µg of mice or human brain lysates diluted in OptiMEM containing lipofectamine 0.8%. After 24 h incubation, cells were fixed with paraformaldehyde 4%, permeabilized using 0.2% Triton X-100 (Sigma-Aldrich, USA,), and incubated in blocking solution (3% horse serum) for 1 h. Cells were then incubated with anti-HA (rabbit, dilution 1:300, cat. 3724 S, Cell Signaling; 2 h RT), and anti-phospho tau AT8 (mouse, dilution 1:300, MN1020, ThermoFisher; overnight at 4 °C) primary antibodies, followed by incubation (2 h, RT) with anti-mouse and anti-rabbit secondary antibodies conjugated to the fluorophores Alexafluor 488 and 647, respectively (dilution 1:500, Invitrogen). Cell nuclei were stained with DAPI (dilution 1:1000, Sigma-Aldrich). Coverslip were mounted on slides with mounting media. Slides were analysed under Zeiss Observer Z1 Microscope (Zeiss, Germany). Images obtained were further analysed using ImageJ software [26].

Statistical analysis

To categorize the individuals according to their seeding profile, the tertile of the seeding sensor response was determined and the population was then segregated into low (normalized RLU sensor signal equals to or lower than 1.11), intermediate (RLU signal between 1.12 and 1.63) or high (RLU signal equals to or higher than 1.64) seeders. The frequency distribution analysis is expressed as percentage of the group population, in order to compensate for the difference in the number of subjects in neurological control and AD groups. All correlation analysis were performed using the nonparametric Spearman test. One outlier of the neurological control group was excluded from the correlation analysis. Heatmap plots were performed after log2 normalization of the variables. For the longitudinal analysis of the evolution of MMSE scores among the 3 tertiles groups of seeding signal, the groups were compared by repeated-measures ANOVA test and by testing the slope of the lines in each group after simple linear regression (patients already at severe AD stage (MMSE < 15 at baseline, $n = 4$) were excluded from this analysis).

The performance of CSF tau seeding in predicting cognitive decline (outcome) was evaluated using multivariate logistic regression model to plot receiver-operating-characteristic (ROC) curves and calculate area under the curves (AUC). The outcome was considered positive [1] in the case of negative delta ≥ 2 between the first and last MMSE scores.

All statistical comparisons were performed using GraphPad Prism software 9. The specific statistical tests used for each experiment are indicated in the figure legends. The significance level was set at $p < 0.05$.

Results

Stratification of AD patients based on tau seeding activity detected in the CSF

We previously developed two biosensors to detect tau seeding properties. One based on the full-length tau harboring the P301L pro-aggregating mutation (tau(P301L)) and another one based on the aggregating-prone region of tau named K18, also mutated at P301L [15]. Tau seeding activity was evaluated in human CSF samples using both, K18(P301L) and tau(P301L), biosensors. The K18(P301L) biosensor signal obtained from all samples were similarly low and close to the basal signal (in the absence of any lysate, normalized value = 1) (Fig. 1A). On the other hand, the tau(P301L) biosensor showed a broad spectrum of signal in response to the CSF samples (Fig. 1B). This high individual variability was expected, as also observed previously in human brain lysate samples

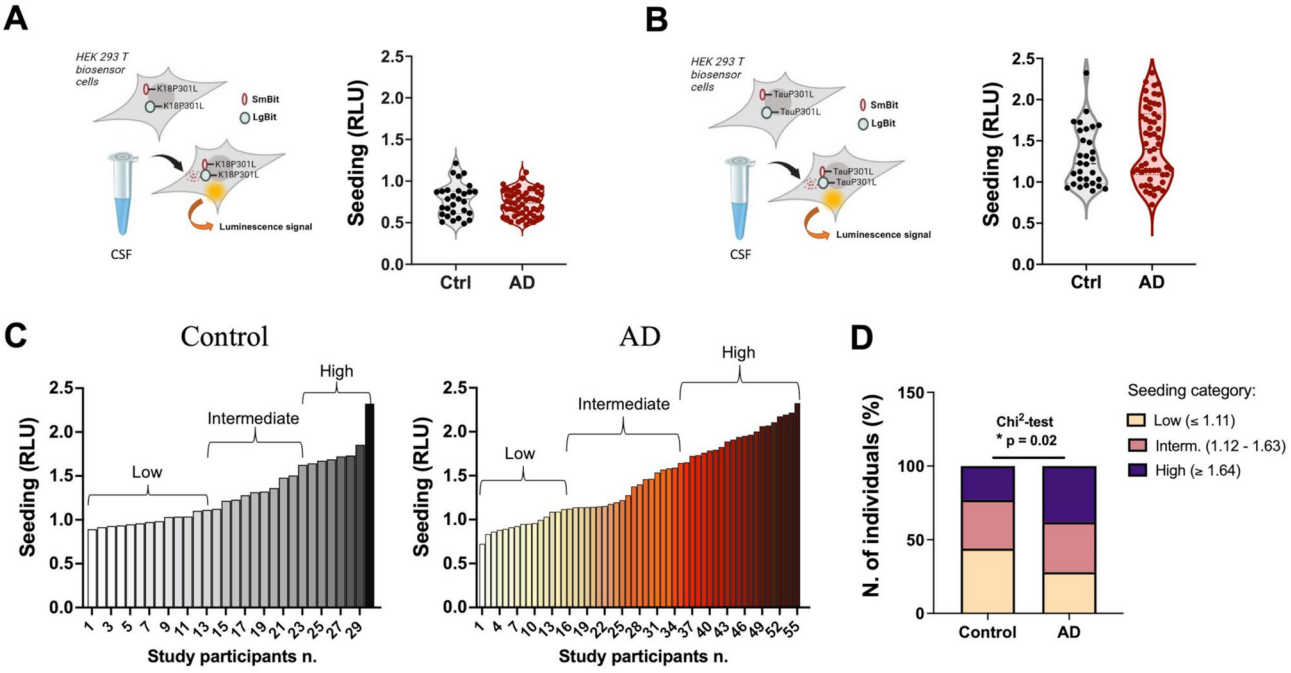

Fig. 1 NanoBit tau biosensor detects seeding activity in human CSF. **A-B)** Violin plot of the signal of K18(P301L) biosensor (**A**) or full-length tau(P301L) biosensor (**B**) cells treated with CSF samples from neurological control (Ctrl) or AD subjects (0.5 µL, 24 h). Data show is normalized to the basal signal (in the absence of any lysate, = 1). **C)** Tau(P301L) biosensor signal for each individual sample shown in B, from neurological control ($n=30$) and AD ($n=55$) groups, ordered by their seeding potency, evidencing the inter-individual variability. **D)** Contingency analysis of the relative proportion of samples displaying low, intermediate or high seeding activity in neurological control and AD groups (χ^2 test, $p=0.02$)

[14]. The following analysis in CSF samples were then performed using the tau(P301L) biosensor. The biosensor signals induced by the CSF from neurological control and AD groups were overlapping, with samples displaying high seeding activity (~1.5–2.5 RLU), and others similar to basal values (~1 RLU), in both groups (Fig. 1C). We then segregated the whole population by the tertiles of the tau(P301L) biosensor signal, and defined three seeding groups, as follow: low ($\leq$ 1.11 RLU), intermediate (1.12–1.63 RLU) and high seeders ($\geq$ 1.64 RLU) (Fig. 1C). When analysing the frequency distribution between neurological controls and AD patients, we observe that the AD group is significantly enriched in subjects displaying high tau seeding activity (χ^2 test, $p=0.026$, Fig. 1D).

Tau seeding activity predicts cognitive decline

We next assessed whether the seeding activity measured in the CSF correlates with the cognitive function. The heatmap plot of MMSE scores at baseline shows an even distribution of subjects displaying all range of scores, from high (>25; good cognitive function) to low (<15; impaired cognitive function) in all three seeding groups (Fig. 2A). A non-significant tendency of negative correlation between the MMSE score and the seeding activity was observed in the neurological control subjects (Fig. 2B), but not in AD patients (Fig. 2C) nor in both groups together (Fig. 2D). In contrast, we detected significant correlations between the MMSE score and AD classical biomarkers measured in the same CSF samples (i.e. positive correlation with CSF-Aβ_{42}; negative correlation with CSF-tau and CSF-phospho-tau (P-tau); Suppl. Figure 1 A-C). Among the 55 AD patients from this study, 34 had one or several follow-up MMSE score measurements within three years. We thus performed longitudinal analysis of the MMSE score progression of those patients, grouped according to the three seeding groups defined above. Interestingly, the rate of cognitive decline was significantly higher in high and intermediate seeders than in low seeders (Fig. 2E). Of note, there were no significant differences in the MMSE score nor in the age of the individuals between the 3 groups at baseline (Suppl. Figure 1D-E). These data suggest that the seeding activity measured in the CSF can be an indicator of short-term (2–3 years) cognitive decline in AD patients, with a low seeding activity indicative of a more stable disease status.

In view of these results, we tested whether the tau seeding activity in the CSF can be of prognostic value to inform on diseases progression probability (cognitive decline as outcome). For this, we compared the area under the receiver operating characteristic curve (ROC) of logistic models to distinguish AD patients who showed cognitive decline from those who remained stable over the time of the study. In our cohort, combining

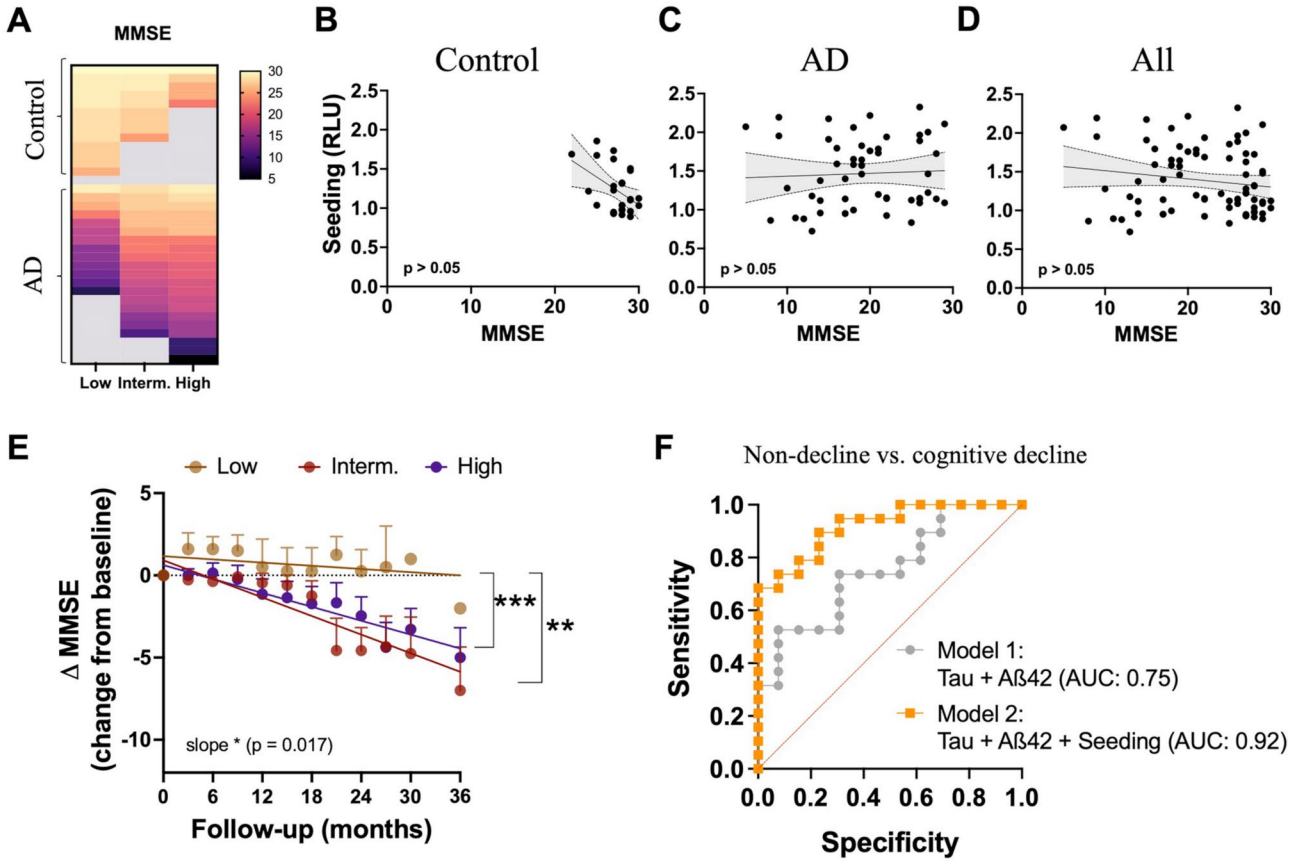

Fig. 2 Correlation between seeding activity and cognitive performance. **A)** Heatmap of cognitive function (MMSE score at baseline) profile in neurological control and AD subjects segregated according to their seeding potency detected in the CSF (high, intermediate or low). **B-D)** Correlation analysis between seeding signal and MMSE score in neurological control (**B**), AD subjects (**C**) or both groups together (**D**). **E)** Longitudinal analysis of cognitive score change (cumulative delta MMSE score to baseline) in each AD subgroup according to the seeding potency (high ($n=14$), intermediate ($n=11$) or low ($n=5$). **F)** Receiver operating curve (ROC) analysis of the predictive model to distinguish AD patients who showed cognitive decline by using tau and Aß$_{42}$ biomarkers only (model 1), or including the seeding activity parameter in the model (model 2). AUC = area under the curve

CSF-total-tau and CSF-Aß$_{42}$ biomarkers gave the best model fit among the classical AD biomarkers tested, with an AUC of 0.75 (Fig. 2F, model 1, 95% CI: 0.58–0.92). Adding the seeding parameter to the model significantly improved its discriminatory value to an AUC of 0.92 (Fig. 2F, model 2, 95% CI: 0.83-1.0). Thus, integrating the seeding response parameter may improve the accuracy of models to discriminate AD patients with an increased likelihood of cognitive decline over the next 2–3 years. Taken together, our data indicate that the AD-related seeding activity can be detected in the CSF and may serve as a prognosis marker for cognitive decline, with interindividual variability potentially contributing to the clinical variability observed in AD progression.

Seeding activity in high seeders is associated with AD classical biomarkers

To gain insight into potential disease-related factors determining the tau seeding activity detected in the CSF, we checked for correlations with the level of classical AD biomarkers measured in the same CSF samples. Heatmap of log2-transformed scaled levels of biomarkers did not show any specific Aß, tau or P-tau signature differences between the three seeding-based subgroups (Fig. 3A). Accordingly, the seeding activity in groups formed based on the A/T profile of biomarkers did not show any differences (Suppl. Figure 2 A). However, correlation analysis within each seeding group revealed some significant associations. In high seeders, the seeding activity does not correlate with Aß$_{42}$ levels (Fig. 3B), but negatively correlates with the Aß$_{42/40}$ ratio, with high seeding activity being observed in those with AD-linked Aß$_{42/40}$ ratios (< 0.08, blue line; Fig. 3C). The seeding activity also positively correlates with tau and P-tau levels in this group (Fig. 3D-E). Seeding activities of intermediate (Fig. 3F-I) and low (Fig. 3J-M) seeders do not correlate with most of the biomarkers tested, with the exception of the low seeders which correlates positively with Aß$_{42}$ levels (Fig. 3J). Of note, in the global population of the study (i.e. without segregating in the three groups of seeding activity)

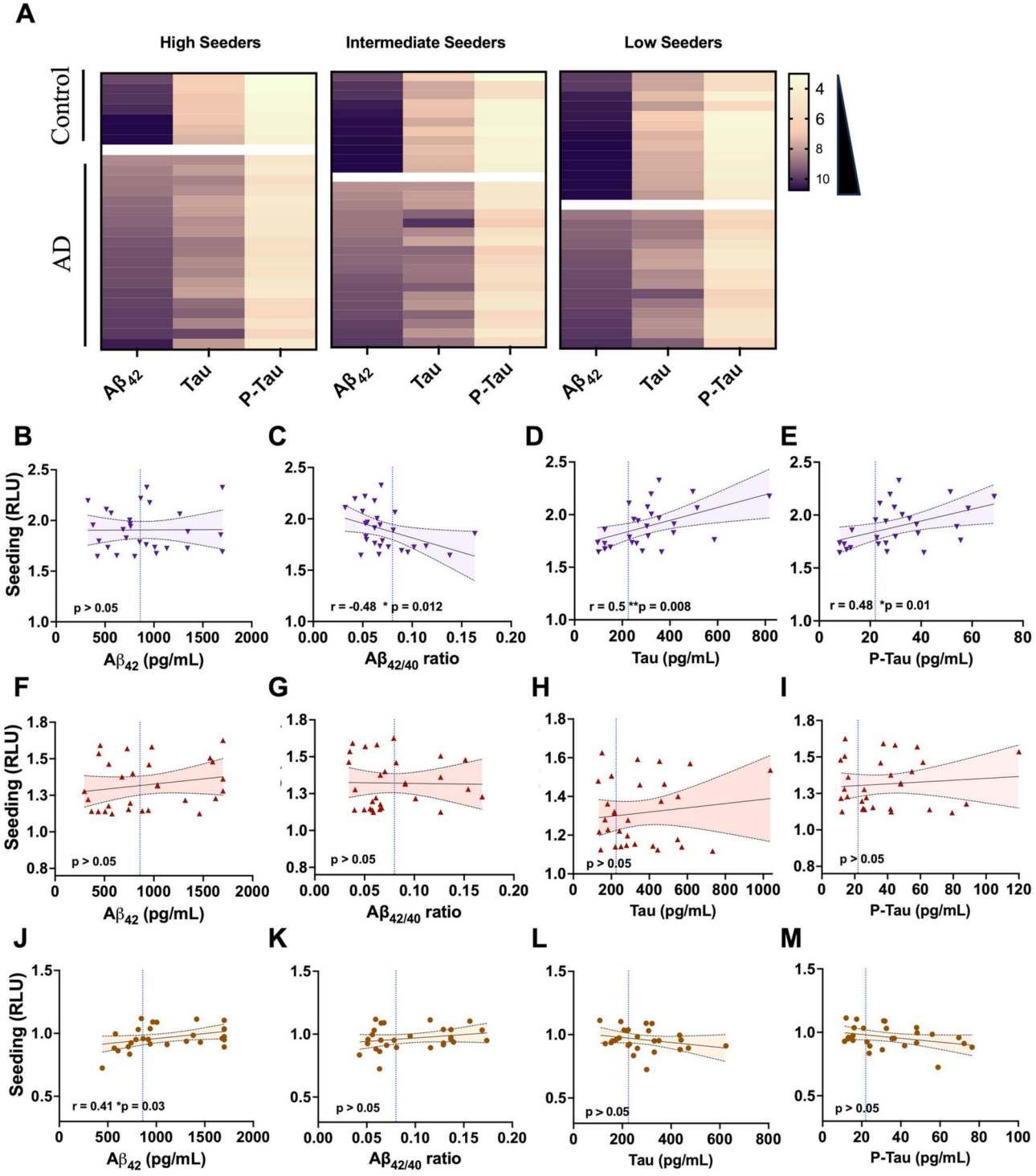

Fig. 3 Correlation between seeding activity and classical AD biomarkers in the CSF. **A)** Heatmap profile of log2-transformed levels (color scale) of classical AD biomarkers in neurological control and AD subjects segregated in three groups accordingly to their seeding potency detected in the CSF: high, intermediate or low seeders. **B-N)** Correlation analysis between seeding signal detected in the CSF using the tau(P301L) biosensor and $Aß_{42}$ levels (**B; F;J**); $Aß_{42/40}$ ratio **(C; G;K)**; total tau **(D; H;L)** and phospho-tau **(E; I;M)** levels in high (**B-E**); intermediate (**F-I**) or low seeders (**J-M**). 95% CI is indicated by the shaded area. Spearman correlation r value and *p* value are indicated when the correlation is statistically significant. Established thresholds for AD diagnosis are indicated by the dotted blue line

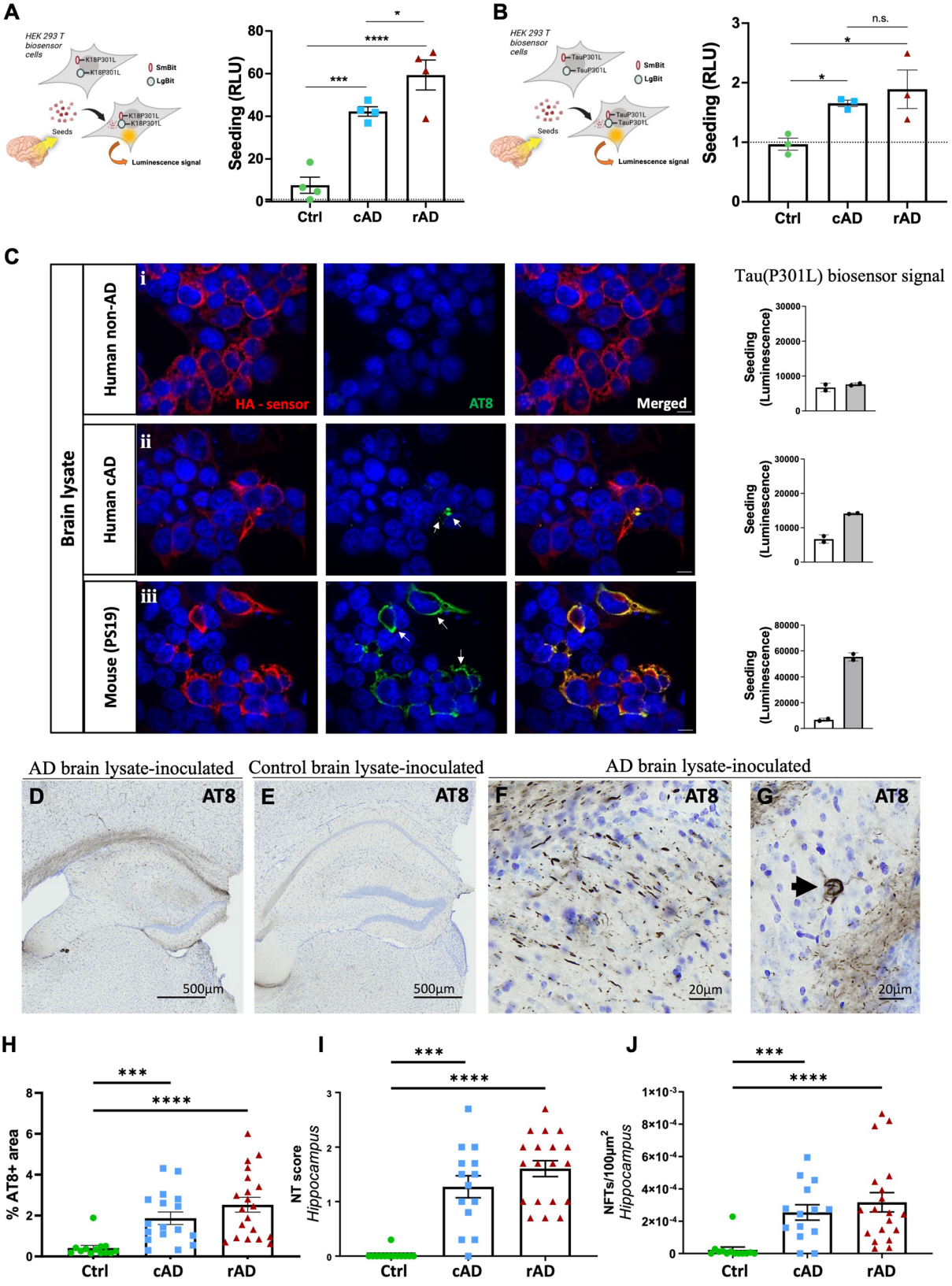

Fig. 4 (See legend on next page.)

(See figure on previous page.)

Fig. 4 NanoBit tau biosensors detect seeding activity in human samples. HEK293T cells expressing the K18(P301L) (**A**) or the full-length tau(P301L) (**B**) biosensor show increased biosensor aggregation in the presence of *post-mortem* human brain lysates (2.5 µg total protein, 24 h) from AD patients compared to control (Ctrl) subjects. cAD = classical AD; rAD = rapid AD (see text for further details). Data are expressed as mean ± SEM of 3–4 independent experiments with the same preparation of homogenates (see Methods for details); *$p < 0.05$, ***$p < 0.005$, ****$p < 0.001$, by one-way ANOVA, followed by uncorrected Dunn's multiple comparisons test to control group. **C)** Representative images of tau biosensor in HEK203T cells incubated in the presence of human or mouse brain lysates, as indicated, monitored by immunofluorescence microscopy (biosensor: anti-HA antibody, in red; AT8 antibody: phospho-tau, in green; nuclei: DAPI staining, in blue). Scale bar: 10 µm. Graphs on the right are the luminescence biosensor data of the corresponding cells (data expressed as mean ± SD of duplicates). **D-J**) Intrahippocampal inoculation of cAD or rAD brain lysates, but not of control brains, increases tau pathology in the hippocampus of $APP_{swe}/PS1_{dE9}$ mice. **D-E)** Representative images of AT8 immunolabelling showing tau pathology induction in the dorsal hippocampus of an AD brain lysate-inoculated $APP_{swe}/PS1_{dE9}$ mouse at 8 mpi (**D**) compared to a control brain-inoculated littermate (**E**). **F-G)** AT8 immunolabelling revealed tau lesions in the forms of neuropil threads (**F**) and NFT (**G**) around the injection site of AD brain-extract-inoculated $APP_{swe}/PS1_{dE9}$ mice at 8mpi. **H-J)** AD brain extract inoculation increased AT8-positive signal (**H**), neuropil threads (**I**) and NFTs (AT8-positive NFTs per 100 μm^2 of area) **(J)** in the hippocampus of AD brain-extract-inoculated $APP_{swe}/PS1_{dE9}$ mice at 8mpi. Scale bars = 500 µm (**D**, **E**), 20 µm (**F–G**). ***$p < 0.001$, ****$p < 0.0001$. nCtrl = 15, n cAD = 15, n rAD = 20 mice. Mann Whitney's tests. Data are shown as mean ± S.E.M. NT = neuropil threads; NFT = neurofibrillary tangles

there was no significant correlation between the seeding activity and any of the biomarkers (Suppl. Figure 2B-E). Therefore, the seeding activity of high seeders (≥ 1.64 RLU) correlates well with the disease context, defined by the three classical AD biomarkers (i.e. decreased $A\beta_{42}/A\beta_{40}$ ratio, increased tau and P-tau).

Based on previous reports in the literature showing that AD patients displaying high tau levels are enriched in subjects carrying the APOE ε4 allele [27], we sought to investigate the distribution of APOE4 carriers in the three seeding groups of our cohort. While in the global population we observed no differences in the frequency of APOE4 + subjects (i.e. carrying at least 1 APOE ε4 allele) among the three groups (Suppl. Figure 2 F), the intermediate and high seeder groups in AD are indeed enriched in APOE4 + subjects (Suppl. Figure 2G). On the contrary, APOE4 + subjects are less abundant in the intermediate and high seeders in the Control group (Suppl. Figure 2 H), evidencing that the seeding detected in the control group is of different nature than that of AD subjects and independent of presence of APOE4 carriers.

Seeding activity in human brain lysates predict their ability to experimentally induce tau pathology in mouse model

To further evaluate the relationship between seeding activity detected with NanoBit tau biosensors and evolution status of patients, we incubated the K18(P301L) or full-length tau(P301L) biosensor cells with *post-mortem* human brain lysates from two clinically distinct groups of sporadic AD patients: one displaying classical progression of the disease ("cAD", defined by a disease duration of 5–8 years) and a group of rapid progression ("rAD"; disease duration from 6 months to 3 years), in addition to non-AD subjects (control). Contrary to the CSF samples, *post-mortem* human brain lysates of AD groups showed a robust increase in the signal of the K18(P301L) biosensor, reaching up to 60-fold changes relative to basal signal (Fig. 4A). In addition, seeding in the rAD sample is statistically higher than in the cAD sample (Fig. 4A). In the case of the tau(P301L) biosensor, the cAD and rAD brain lysates induced a significant increase in the signal compared to brain lysates from control subjects (Fig. 4B), with a similar amplitude than that observed with the CSF samples. However, no significant difference was observed between the cAD and rAD brain lysates (Fig. 4B). These data further suggests that K18(P301L) and tau(P301L) biosensors detect different seeding processes, with the tau(P301L) biosensor displaying more concordance between brain lysate and CSF samples.

We have previously shown that seeding induced by brain lysates from the P301S transgenic mouse model of tauopathy leads to AT8-positive staining of the tau(P301L) biosensor, which correlates well with the biosensor signal [15, 28]. Here we assessed whether this is also the case with the *post-mortem* human brain lysates. Confocal imaging of tau(P301L) biosensor cells show absence of AT8 staining in cells incubated with control non-AD human brain lysates (Fig. 4C-i), while incubation with cAD brain lysates show some AT8-positive speckle-shaped tau inclusions (Fig. 4C-**ii**). In contrast, the majority of tau biosensor molecules are phosphorylated (AT8-positive) following treatment with brain lysates from the P301S mouse model (PS19), used as a positive control (Fig. 4C-**iii**). The level of AT8-positive phosphorylation seems thus to correlate well with the biosensor aggregation signal (Fig. 4C, **graphs on the right**), confirming our previous data [15, 28]. Morphological differences and heterogeneity of AT8-positive inclusions driven by human vs. mouse brain lysates (see Suppl. Figure 3 A-B for higher magnification images) might explain the differences in the amplitude of the biosensor response towards those samples, and might reflect different seed structures, strain properties or seed-substrate compatibility.

Finally, in order to confirm that the biosensor response is related to the pathological properties of the seeds contained in the samples, we assessed the capacity of these human samples to induce tau pathology in vivo. For this, we used a previously validated APP/PS1dE9 mouse model that do not overexpress pathological tau proteins but that over-express amyloid-beta peptide, known to boost tau seeding activity [29], [30]. Compared to the

control brain lysate, the intrahippocampal inoculation of both cAD and rAD brain lysates led to a similar significant increase in tau lesions in the hippocampus, as revealed by AT8-positive immunostaining (Fig. 4D-E and H; $p = 0.001$ and $p < 0.0001$ respectively for cAD and rAD-inoculated mice). AT8-positive neuropil threads (NTs) in the hippocampus were also induced in a similar way for both cAD and rAD (Fig. 4F and I; $p = 0.0005$ and $p < 0.0001$ in cAD and rAD mice, respectively), whereas control-inoculated animals did not present these lesions. Moreover, AT8-positive neurofibrillary tangles (NFTs) were also increased in a similar way for the two AD groups in the hippocampal hilus (Fig. 4G and J; $p = 0.001$ and $p < 0.0001$ in cAD and rAD mice, respectively) as opposed to control-inoculated animals. Tau lesions spreading from the hippocampus to entorhinal region were also detected and occurred with the same intensity after cAD and rAD inoculation (not shown). Altogether these data demonstrate that the NanoBit tau biosensors are efficient in detecting seeding activity in human biological samples that are pathologically relevant, as demonstrated by their induction of tau pathology in mice upon brain inoculation of the same samples.

Discussion

Tau seeding and replication activities are considered the key prion-like mechanisms through which tau pathology propagates from one cell to another, eventually spreading through different brain regions over the course of AD progression [8]' [7]. While seeding-active tau species have been extensively shown from human *postmortem* brain tissue lysates in previous studies [11, 14, 17, 31], the detection of seeding-active tau species in the CSF is much more challenging, likely due to the low amounts of tau species in this fluid. Here, we applied recently developed tau biosensors based on the NanoBit technology to detect tau seeding activity from *antemortem* CSF samples, as well as *postmortem* brain lysates. The tau seeding activity from *postmortem* brain lysates could clearly discriminate AD from non-AD subjects using K18(P301L) and tau(P301L) biosensors. In contrast, tau seeding activity from CSF samples was only detectable with the tau(P301L) biosensors and in both, AD and neurological control subjects, with similar high inter-individual variability inside the two groups. Subjects classified as "high seeders" were more abundant in the AD group, and their seeding response correlated with classical AD biomarkers, implying that high seeding activity in the CSF is linked to the disease context. Further evidence of the relevance of the tau seeding detected in the CSF of AD subjects comes from the observation that the group of high seeders in AD, but not in Control, is enriched in APOE4 carriers.

The most striking observation is that seeding activity measured in the CSF might be a useful parameter to report on the dynamic phase of AD progression. Indeed, subjects with low seeding activity showed clearly slower cognitive decline in the following 30 months. Provided that our findings are confirmed in additional cohorts, they could have meaningful clinical translational benefits for patient stratification, especially in view of the recent approval of the 2 first disease-modifying drugs for AD patients [32]. Being able to identify patients that are at low risk to decline cognitively in the next couple of years will certainly be an asset for clinicians to prevent therapy initiation in subjects that will not benefit from them. Similarly, being able to discriminate low and fast decliners may also be critical to refine patient recruitment in clinical trials.

Interestingly, full length tau(P301L) and K18(P301L) biosensors showed different results in CSF and *post-mortem* brain lysate samples, with the full-length tau(P301L) biosensor being better suited to detect tau seeding in CSF samples. These results strongly suggest that the seeding-competent species are not the same in *postmortem* brain lysates and in *antemortem* CSF, although a contribution of different seed levels (i.e. high in brain lysates and low in CSF) cannot be fully discarded. In fact, a previous study reported that the tau species found in the brain and CSF of living healthy subjects are indeed not identical, with the CSF being enriched in N terminus fragments cleaved at the end of the mid-domain between residues 222 and 225, lacking thus the central repeat K18 domain [33]. Such species might, therefore, display seeding activity on full-length tau constructs, but not on K18-only constructs. Interestingly, according to the authors, the profile of CSF tau fragments is very similar in AD and non-AD subjects, with the main difference being the increased production rate of tau in the former [33]. This might explain why we also detect seeding activity in the CSF of neurological control subjects. Whether this phenomenon relates to a yet unknown physiological function of secreted tau remains to be explored. Another evidence attesting for different seeding-competent species in human brain lysates compared to the CSF of AD patients is the fact that the seeding potency seems to correlate with the levels of distinct phosphorylated tau species. While in the CSF the seeding potency is, at least, correlated with T181 p-tau (our study), in human brain lysates it correlates with tau species phosphorylated at residues T231 and S235, but not with the T181 p-tau [14]. Future studies will have to investigate relationships between CSF seeding potency and tau species phosphorylated at other residues, including T231 and S235, both of which have been shown to be of high relevance as biomarkers of early AD [34]. Of note, only one study, led by Takeda et al.., had previously reported successful

detection of tau seeding activity in *antemortem* human CSF, using a K18-based FRET biosensor cells combined to specific CSF sample preparation to obtain 50-times concentrated high molecular weight tau fractions [16]. Among the 6 AD samples tested, seeding was detected only in 3 of them, which proves that seeding-competent tau species can be indeed found in the CSF, but also implies high inter-individual variability of seeding activity. Both aspects are now corroborated by our results in a larger set of samples. Further evidence of the presence of seeding-competent tau species in the human CSF also comes from studies that successfully induced tau pathology in the mice brain after inoculating human CSF from AD cases [35]. More recently, Hitt et al.. reported that an optimized version of the FRET biosensor could not detect tau seeding activity in human CSF [17]. The discrepancy between the two studies [16]' [17] is most likely due to differences in the protocol of sample preparation. In our case, our results showing that only few samples had detectable signal above the basal line (Fig. 1A), using the K18-based NanoBit biosensors (similar construct to the one used in the FRET biosensor), are in good agreement with those of the study from Hitt and collaborators.

Recently developed in vitro seed-amplification assays ((SAA), or Real-Time quaking induced conversion assay (RT-QuIC)) have shown promising results in the case of alpha-synucleinopathies, displaying high sensitivity and specificity in detecting seed-competent alpha-synuclein in the CSF of Parkinson's and Lewy bodies diseases patients, even at presymptomatic stages [36, 37]. Detection of tau seeds by similar assays revealed to be, however, more challenging, probably due to the higher complexity of isoforms and conformations of tau compared to alpha synuclein. In AD, successful results have been up to now reported in *postmortem* brain samples only [13, 38]. It is interesting to highlight that, in more concentrated samples, these assays also detect tau seeding in non-AD brain specimens [13, 38], supporting the existence of some degree of basal seeding activity. Of note, in our previous study [15] we compared side-by-side our biosensor signal and thioflavin staining the biosensor cells, and we observed no correlation, suggesting that the biosensor signal reflects oligomeric complexes rather than fibrillar forms of tau, which might explain the higher sensibility of the sensor and the signal from control CSF samples.

The well-characterized cohort used in the present study enabled us to relate tau seeding activity to clinical and biomarker parameters. In AD subjects with high seeding activity profile, the seeding potency correlates negatively with $Aß_{42/40}$ ratio, and positively with total- and p-tau, highlighting its connection to the progression of AD biomarkers. Of note, we [15] and others [9] did not observe a direct effect of Aß oligomers on inducing tau aggregation, but it is very likely that Aß pathology contributes indirectly to aggravate tau lesions. The positive correlation of seeding activity with total- and P-tau181 could suggest that these are critical factors determining seeding activity. However, they are certainly not the only factors, as subjects with similarly high tau and P-tau181 levels were also present in the group of low and intermediate seeders. Thus, in addition to total-tau and P-tau181 levels, the seeding activity presumably reflects other pro-seeding properties of CSF samples, either from the presence other P-tau species, such as P-tau231 which can be increased in non-AD cases, as in chronic traumatic encephalopathy [39] for example, or from still to be discovered factors unrelated to tau. In this same line, the study from Duits and collaborators [27] highlighted the fact that higher tau levels are associated with faster cognitive decline independently of the disease stage, which suggests that different underlying biological process might drive the four AD subgroups they discovered, as well as the seeding subgroups reported here. The APOE genotype is another potential factor modulating tau levels heterogeneity [14, 27] and seeding activity, as we found that the group of intermediate and high seeders among AD subjects are enriched in APOE4 carriers, compared to low seeders.

It is, therefore, highly plausible that tau seeding activity may significantly contribute to the clinical heterogeneity observed on AD progression. This hypothesis has also been suggested in the study from Dujardin and collaborators [14] upon identification of significant variability on several post-translational modifications of tau and seeding properties in soluble high molecular weight brain fraction of human *postmortem* frontal cortices. Of note, the authors observed a positive correlation between seeding activity and the rate of disease progression, and the inoculation of human brain samples into the brain of AD animal models also induced tau pathology proportional to the seeding potency of the human sample [14], which is in agreement with our data.

The present work has some limitations that should be acknowledged. We did not explore the response of the seeding biosensor in samples from young, healthy subjects, or from other neurodegenerative diseases, especially other 4R tauopathies (PSP, CBD). The inclusion criteria of control subjects were limited, as they were also referred to the memory clinic due to cognitive complaints. Because the CSF samples were not assessed for other potential co-pathologies, the possibility of cross-seeding by other aggregate species cannot be entirely excluded. Further studies in a different and larger cohort, with available cognitive data on additional tests, in particular ADAS-cog and CDR-SB, as well as with data on other P-tau species and tau PET scan, are warranted to increase the robustness of our conclusions and to better

understand the relationship between CSF seeding activity and AD pathophysiology. Larger cohorts will also allow correlations with demographic markers such as age, sex and years of education with sufficient statistical power. Finally, future studies should address the application of the seeding biosensor to serum or plasma samples to fully explore its translational potential as a routine assay.

Conclusion

In summary, we report here that seeding activity is a parameter that can be detected in the CSF by a full-length Tau(P301L) NanoBit-based biosensor. CSF seeding activity is highly heterogeneous among AD and non-AD subjects, but in diagnosed AD cases it might predict the probability of cognitive decline in the short-term. Confirmation of these findings and testing the predictive model in larger and independent cohort are likely to pave the way for integrating seeding activity as a new biomarker in AD research as well as in clinical practice, allowing better patient selection for treatment indication and/or inclusion in clinical trials.

Abbreviations

Aß	Amyloid beta
AD	Alzheimer disease
AUC	Arear under the curve
cAD	Classical AD
rAD	Rapid AD
CSF	Cerebrospinal fluid
MMSE	Mini Mental State Examination
P-tau	Phosphorylated tau
RLU	Relative Luminescence Signal

Supplementary Information

The online version contains supplementary material available at https://doi.org/10.1186/s13195-025-01792-w.

Supplementary Material 1

Acknowledgements

The authors are grateful to all donors, patients and their families. We acknowledge all members of the respective laboratories for stimulating discussions and comments on the project. We acknowledge the Brainbank Neuro-CEB Neuropathology Network, Charles Duyckaerts and Susana Boluda for providing the brain samples. We acknowledge Sabiha Eddarkaoui and Luc Buée for biochemical analysis of the human brain samples. We acknowledge Anne-Sophie Hérard for support in the follow-up of mouse experiment analysis. We thank Martine Guillermier and Mylène Gaudin for surgical expertise during inoculation of brain extracts to animals. We thank the Brain Donation Program of the NeuroCEB Brainbank Neuropathologist's Network, with the support of Fondation Plan Alzheimer and IHU A-ICM for providing the brain samples used in this study. We thank Fany Panayi for providing the brain lysates of the PS19 transgenic mouse model. We thank the IMAG'IC core facility of Institute Cochin (Paris, France) for their support.

Author contributions

J.D., R.J. and E.C. conceived and designed experiments. M.D., S.L., F.P. contributed to the mouse study conception and design. S.H. provided the rAD brain extracts. F.P. and S.L. designed and performed the immunohistological analysis in animals. L.H. and E.C. performed the biosensor tests, cell immunostaining and data analysis. F.M.L., J.H. and C.P. performed biomarker quantification of the CSF samples and clinical analysis. J.D., R.J. and E.C. contributed to data analysis. M.D., J.H., C.P., R.J. and E.C. obtained the funding. E.C., M.D. and R.J. wrote the manuscript that was edited and/or approved by all authors.

Funding

This work was supported by the Agence Nationale de la Recherche (ANR-23-CE18-0008 SENS-AD, to E.C.), the Fondation de la Recherche Médicale (MND202310017920, to E.C.), Institut National de la Santé et de la Recherche Médicale (INSERM), Centre National de la Recherche Scientifique (CNRS) and by the French Government through its "Investments for the Future" program–Idex ("Tau-sens") operated by the Paris University (to J.H. and R.J).

Data availability

No datasets were generated or analysed during the current study.

Declarations

Ethics approval and consent to participate

All animal experimental procedures were conducted in accordance with the European Community Council Directive 2010/63/UE and approved by local ethics committees (CEtEA-CEA DSV IdF N°44, France) and the French Ministry of Education and Research (A17_083 authorization), and in compliance with the 3R guidelines. The human CSF samples were collected at the Center of Cognitive Neurology, Lariboisière Hospital with approval by the Ethical Committee of Paris Diderot University Hospitals (CEERB Bichat University Hospital, Paris, France). The human brain lysates were collected from a brain donation program of the NeuroCEB and the CNR-prion brain banks. Consent forms were previously signed by either the patients themselves or their next of kin, in accordance with French bioethics laws.

Consent for publication

Not applicable.

Competing interests

The authors declare no competing interests.

Received: 14 April 2025 / Accepted: 20 June 2025
Published online: 02 July 2025

References

1. Cummings J, Lee G, Ritter A, Zhong K. Alzheimer's disease drug development pipeline: 2018. Alzheimers Dement (N Y). 2018;4:195–214.
2. Jack CR, Bennett DA, Blennow K, Carrillo MC, Feldman HH, Frisoni GB, et al. A/T/N: an unbiased descriptive classification scheme for alzheimer disease biomarkers. Neurology. 2016;87(5):539–47.
3. Jack CR Jr., Knopman DS, Jagust WJ, Shaw LM, Aisen PS, Weiner MW, et al. Hypothetical model of dynamic biomarkers of the alzheimer's pathological cascade. Lancet Neurol. 2010;9(1):119–28.
4. Jack CR Jr., Bennett DA, Blennow K, Carrillo MC, Dunn B, Haeberlein SB, et al. NIA-AA research framework: toward a biological definition of alzheimer's disease. Alzheimers Dement. 2018;14(4):535–62.
5. Goedert M, Masuda-Suzukake M, Falcon B. Like prions: the propagation of aggregated Tau and alpha-synuclein in neurodegeneration. Brain. 2017;140(2):266–78.
6. Braak H, Braak E. Neuropathological stageing of Alzheimer-related changes. Acta Neuropathol. 1991;82(4):239–59.
7. Jagust W. Imaging the evolution and pathophysiology of alzheimer disease. Nat Rev Neurosci. 2018;19(11):687–700.
8. Jucker M, Walker LC. Self-propagation of pathogenic protein aggregates in neurodegenerative diseases. Nature. 2013;501(7465):45–51.
9. Holmes BB, Furman JL, Mahan TE, Yamasaki TR, Mirbaha H, Eades WC, et al. Proteopathic Tau seeding predicts Tauopathy in vivo. Proc Natl Acad Sci U S A. 2014;111(41):E4376–85.
10. DeVos SL, Corjuc BT, Oakley DH, Nobuhara CK, Bannon RN, Chase A, et al. Synaptic Tau seeding precedes Tau pathology in human alzheimer's disease brain. Front Neurosci. 2018;12:267.
11. Furman JL, Vaquer-Alicea J, White CL 3rd, Cairns NJ, Nelson PT, Diamond MI. Widespread Tau seeding activity at early Braak stages. Acta Neuropathol. 2017;133(1):91–100.

12. Kaufman SK, Del Tredici K, Thomas TL, Braak H, Diamond MI. Tau seeding activity begins in the transentorhinal/entorhinal regions and anticipates phospho-tau pathology in alzheimer's disease and PART. Acta Neuropathol. 2018;136(1):57–67.
13. Kraus A, Saijo E, Metrick MA 2nd, Newell K, Sigurdson CJ, Zanusso G, et al. Seeding selectivity and ultrasensitive detection of Tau aggregate conformers of alzheimer disease. Acta Neuropathol. 2019;137(4):585–98.
14. Dujardin S, Commins C, Lathuiliere A, Beerepoot P, Fernandes AR, Kamath TV, et al. Tau molecular diversity contributes to clinical heterogeneity in alzheimer's disease. Nat Med. 2020;26(8):1256–63.
15. Cecon E, Oishi A, Luka M, Ndiaye-Lobry D, Francois A, Lescuyer M et al. Novel repertoire of Tau biosensors to monitor pathological Tau transformation and seeding activity in living cells. Elife. 2023;12.
16. Takeda S, Commins C, DeVos SL, Nobuhara CK, Wegmann S, Roe AD, et al. Seed-competent high-molecular-weight Tau species accumulates in the cerebrospinal fluid of alzheimer's disease mouse model and human patients. Ann Neurol. 2016;80(3):355–67.
17. Hitt BD, Vaquer-Alicea J, Manon VA, Beaver JD, Kashmer OM, Garcia JN, et al. Ultrasensitive Tau biosensor cells detect no seeding in alzheimer's disease CSF. Acta Neuropathol Commun. 2021;9(1):99.
18. Lam S, Herard AS, Boluda S, Petit F, Eddarkaoui S, Cambon K, et al. Pathological changes induced by alzheimer's brain inoculation in amyloid-beta plaque-bearing mice. Acta Neuropathol Commun. 2022;10(1):112.
19. Lam S, Petit F, Herard AS, Boluda S, Eddarkaoui S, Guillermier M, et al. Transmission of amyloid-beta and Tau pathologies is associated with cognitive impairments in a primate. Acta Neuropathol Commun. 2021;9(1):165.
20. Lilamand M, Bouaziz-Amar E, Dumurgier J, Cognat E, Hourregue C, Mouton-Liger F, et al. Plasma leptin is associated with amyloid CSF biomarkers and alzheimer's disease diagnosis in cognitively impaired patients. J Gerontol Biol Sci Med Sci. 2023;78(4):645–52.
21. du Sert NP, Hurst V, Ahluwalia A, Alam S, Altman DG, Avey MT, et al. Revision of the ARRIVE guidelines: rationale and scope. BMJ Open Sci. 2018;2(1):e000002.
22. Gary C, Lam S, Herard AS, Koch JE, Petit F, Gipchtein P, et al. Encephalopathy induced by alzheimer brain inoculation in a non-human primate. Acta Neuropathol Commun. 2019;7(1):126.
23. Paxinos GFK. The mouse brain in stereotaxic coordinates. Cambridge: Academic; 2001.
24. Dixon AS, Schwinn MK, Hall MP, Zimmerman K, Otto P, Lubben TH, et al. NanoLuc complementation reporter optimized for accurate measurement of protein interactions in cells. ACS Chem Biol. 2016;11(2):400–8.
25. Lee G, Neve RL, Kosik KS. The microtubule binding domain of Tau protein. Neuron. 1989;2(6):1615–24.
26. Schneider CA, Rasband WS, Eliceiri KW. NIH image to imageJ: 25 years of image analysis. Nat Methods. 2012;9(7):671–5.
27. Duits FH, Wesenhagen KEJ, Ekblad L, Wolters E, Willemse EAJ, Adni, et al. Four subgroups based on Tau levels in alzheimer's disease observed in two independent cohorts. Alzheimers Res Ther. 2021;13(1):2.
28. Amorim IS, Challal S, Cistarelli L, Dorval T, Abjean L, Touzard M, et al. A seeding-based neuronal model of Tau aggregation for use in drug discovery. PLoS ONE. 2023;18(4):e0283941.
29. He Z, Guo JL, McBride JD, Narasimhan S, Kim H, Changolkar L, et al. Amyloid-beta plaques enhance alzheimer's brain Tau-seeded pathologies by facilitating neuritic plaque Tau aggregation. Nat Med. 2018;24(1):29–38.
30. Vergara C, Houben S, Suain V, Yilmaz Z, De Decker R, Vanden Dries V, et al. Amyloid-beta pathology enhances pathological fibrillary Tau seeding induced by alzheimer PHF in vivo. Acta Neuropathol. 2019;137(3):397–412.
31. Saijo E, Metrick MA 2nd, Koga S, Parchi P, Litvan I, Spina S, et al. 4-Repeat Tau seeds and templating subtypes as brain and CSF biomarkers of frontotemporal Lobar degeneration. Acta Neuropathol. 2020;139(1):63–77.
32. Selkoe DJ. The advent of alzheimer treatments will change the trajectory of human aging. Nat Aging. 2024;4(4):453–63.
33. Sato C, Barthelemy NR, Mawuenyega KG, Patterson BW, Gordon BA, Jockel-Balsarotti J, et al. Tau kinetics in neurons and the human central nervous system. Neuron. 2018;97(6):1284–98. e7.
34. Lantero-Rodriguez J, Snellman A, Benedet AL, Mila-Aloma M, Camporesi E, Montoliu-Gaya L, et al. P-tau235: a novel biomarker for staging preclinical alzheimer's disease. EMBO Mol Med. 2021;13(12):e15098.
35. Skachokova Z, Martinisi A, Flach M, Sprenger F, Naegelin Y, Steiner-Monard V, et al. Cerebrospinal fluid from alzheimer's disease patients promotes Tau aggregation in Transgenic mice. Acta Neuropathol Commun. 2019;7(1):72.
36. Shahnawaz M, Tokuda T, Waragai M, Mendez N, Ishii R, Trenkwalder C, et al. Development of a biochemical diagnosis of Parkinson disease by detection of alpha-Synuclein misfolded aggregates in cerebrospinal fluid. JAMA Neurol. 2017;74(2):163–72.
37. Palmqvist S, Rossi M, Hall S, Quadalti C, Mattsson-Carlgren N, Dellavalle S, et al. Cognitive effects of lewy body pathology in clinically unimpaired individuals. Nat Med. 2023;29(8):1971–8.
38. Frey B, Holzinger D, Taylor K, Ehrnhoefer DE, Striebinger A, Biesinger S, et al. Tau seed amplification assay reveals relationship between seeding and pathological forms of Tau in alzheimer's disease brain. Acta Neuropathol Commun. 2023;11(1):181.
39. Turk KW, Geada A, Alvarez VE, Xia W, Cherry JD, Nicks R, et al. A comparison between Tau and amyloid-beta cerebrospinal fluid biomarkers in chronic traumatic encephalopathy and alzheimer disease. Alzheimers Res Ther. 2022;14(1):28.

Publisher's note